

Scanning Tunneling Microscopy Study of Poly-L-Proline

Carl Rau¹, Nanjiu Zheng¹, Carlton Hazlewood²
and Gert Rau²

¹Department of Physics and Rice Quantum Institute, Rice University, Houston, Texas
and ²Department of Molecular Physiology and Biophysics, Baylor School of Medicine, Houston, Texas

Abstract: Differences in its peptide bonds allow the imino acid poly-L-proline to exist in two significantly different geometric structures. Form I with *cis* peptide bonds is supposed to be a right-handed helix and form II with *trans* peptide bonds a left-handed helix. *Cis/trans* isomerization about the proline imide is believed to cause the denaturation of a number of proteins and may be a key step in protein folding. Using scanning tunneling microscopy (STM), we present high-resolution images of air-dried poly-L-proline. It is found that the electric conductivity of one monolayer of poly-L-proline is sufficient to allow for STM imaging without significant tip-sample interaction. Only at locations where stacking of poly-L-proline chains occurs, a direct contact of the probing tip to the molecules becomes apparent and prevents us, at present, from resolving the atomic structure of the topmost layer. Our STM images of poly-L-proline show that form II is relatively rigid and forms aggregates in most cases. Form I, which is occasionally observed, is very flexible and exhibits sharp bends as well as 180° backfolding. These observations confirm theoretical predictions on the existence of two peptide bond conformations of poly-L-proline.

SCANNING TUNNELING MICROSCOPY (STM) is capable of providing real space and three-dimensional images of surfaces with atomic resolution in both ultra high vacuum (UHV) and in ambient environment. In the past few years, STM has achieved a tremendous success in elucidating the atomic structure of semiconductor surfaces. STM is now emerging as an important new technology for biological applications and offers much promise for high-resolution imaging of cellular and molecular structures. Even though, at present, there is no complete understanding of the electron tunneling mechanism in biological samples, a series of biomolecules has already been imaged successfully (1-4). The further application of STM in this area relies on the understanding of contrast formation in STM imaging, as well as on the availability of reliable and reproducible experimental data. One way to achieve this is imaging of samples of which the basic structures are well understood.

The imino acid proline is an important structural determinant in proteins. Among 20

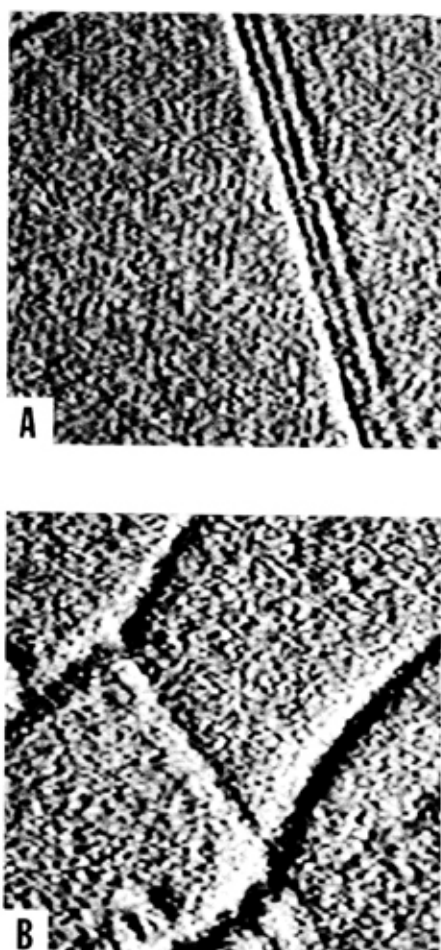


FIGURE 1. Edge-detected STM images showing artifacts observed at the surface of graphite substrates. The images are of dimensions of (a) $(5600 \times 5600) \text{ \AA}^2$ and (b) $(3500 \times 3500) \text{ \AA}^2$. The tunneling current was 0.3 nA, and the tip voltage was +100 mV.

different amino acids, only proline has the side chain covalently bonded to the nitrogen atom of the peptide group, thus forming a cyclic α -imino-acid ring which imposes severe steric constraints on the rotation of the N-C bond. Early investigations, using X-ray diffraction, infrared absorption, Raman spectroscopy, electron microscopy and nuclear magnetic resonance, (5–10) showed that there exist two conformational structures of poly-L-proline, referred to as form I and form II. Poly-L-proline I, exhibiting a specific rotation of $+40^\circ$ in water, is a right-handed helix with all peptide bonds in *cis* configuration, and poly-L-proline II, exhibiting a specific rotation of -540° , is a left-handed helix with all peptide bonds in *trans* configuration. The ^{13}C - and H-NMR experiments demonstrated that mutarotation between form I and II occurs over a period of several days when poly-L-proline is dissolved in appropriate solvents.

The purpose of the present study is to determine whether poly-L-proline can be imaged with STM and to what degree direct evidence on the existence of two conformations of poly-L-proline can be confirmed using topographic STM imaging.

Materials and Methods

Synthetic poly-L-proline powder (molecular weight: 1,000–10,000) was purchased from the Sigma Chemical company. Its specific rotation in water is -446° . All samples for STM imaging were prepared by dissolving poly-L-proline powder in 0.1 mol NaH_2PO_4 solvent at a concentration of 5 w.-% and depositing a small amount of this solution onto a (0001)-oriented surface of freshly cleaved, highly-oriented pyrolytic graphite (HOPG). The samples were air dried in a desiccator for two days, and then they were transferred to perform STM.

The microscope will be described in detail elsewhere. Here we give a brief description. A commercial inchworm (Burleigh Instruments) is used to move the sample towards the probing tip to within a working distance of 10 Å where the electronic feedback takes control of the STM imaging. The images are acquired by scanning a piezoelectric tube, on which the tip is mounted at the center, across the sample. The maximum scanning area is about $3 \mu\text{m} \times 3 \mu\text{m}$. The tube scanner is calibrated, using atomically-resolved STM images and also images of optical diffraction gratings and surface steps, to lateral and vertical accuracies of 2% and 7%, respectively. All images presented here, are acquired using constant-current mode and a line scan rate of about 1 Hz.

The HOPG (0001) surface is known to be atomically flat up to a few microns along the surface and is widely used as a substrate for biological applications. We note, however that recent studies show that HOPG substrates may introduce artifacts which mimic the shape of certain biomolecules (11) and thus could complicate the reliable interpretation of STM images. Therefore, we examined a large number of uncovered graphite surfaces and found that these artifacts are associated with surface steps and long straight line features. Two examples of such artifacts are shown in Figure 1. These features are usually very long and totally different from those of poly-L-proline molecules we present in the following section.

Results and Discussion

High-quality STM images of uncoated poly-L-proline molecules were obtained by using small, positive tip voltages, typically less than 0.5 V and tunneling currents of about 0.3 nA. We note that increasing the tip voltage up to 1 V or higher resulted in an occurrence of noise in the tunneling current being present only at the location of poly-L-proline molecules. In addition, we found that using such high voltages, certain poly-L-proline features deteriorated after several STM scans. This, we believe, indicates the influence of electric fields on the molecules.

Figure 2 shows a typical and also characteristic, low-magnification STM image of poly-L-proline molecules. In order to highlight certain poly-L-proline features, we present our STM images in the first derivative mode. In the following, we refer to these images as edge-detected and to original STM data as gray-scale images. In Figure 2, aggregates of poly-L-proline molecules are clearly visible. The overall lateral size of these aggregates is

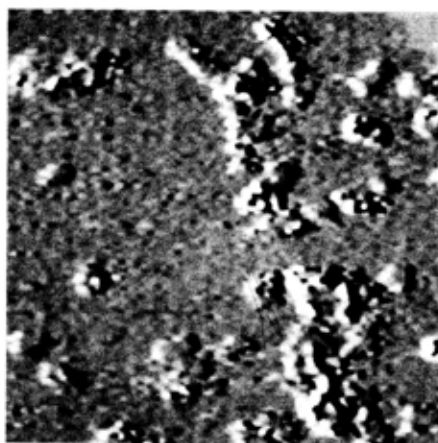


FIGURE 2. Edge-detected STM image of $(2800 \times 2800) \text{ \AA}^2$ showing poly-L-proline aggregates. The size of the aggregates is about 500 \AA in diameter. The tunneling current was 0.5 nA , and the tip voltage was $+150 \text{ mV}$.

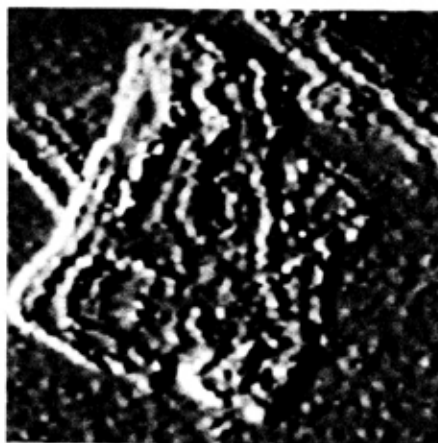


FIGURE 3. High resolution, edge-detected STM image $(900 \times 900) \text{ \AA}^2$ showing poly-L-proline aggregates stacked on top of the other. The periodic structure consisting of parallel-linked polypeptide chains can be seen at the "bottom" aggregate. The distance between two neighboring chains is about 25 \AA . The tunneling current was 0.3 nA , and the tip voltage was $+150 \text{ mV}$.

of the order of 500 \AA . We note that a few larger aggregates are also visible. These, however, predominantly consist of an array of randomly-stacked small aggregates.

Figure 3 gives a magnified, edge-detected STM image of one of these larger aggregates. We clearly can identify two smaller aggregates. It is interesting to note that these smaller aggregates are very regular in shape, where one of them even shows a periodic line structure.

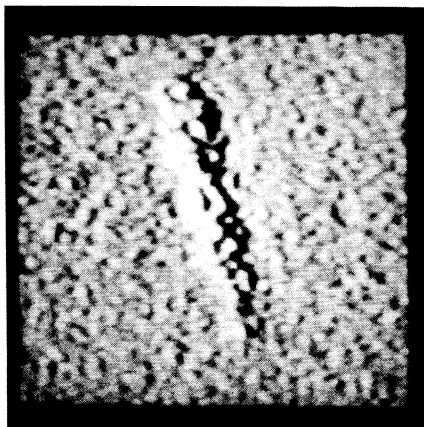


FIGURE 4A. Low magnification edge-detected STM image (420×420) \AA^2 of one structure in the sample. The tunneling current was 0.5 nA, and the tip voltage was 150 mV.

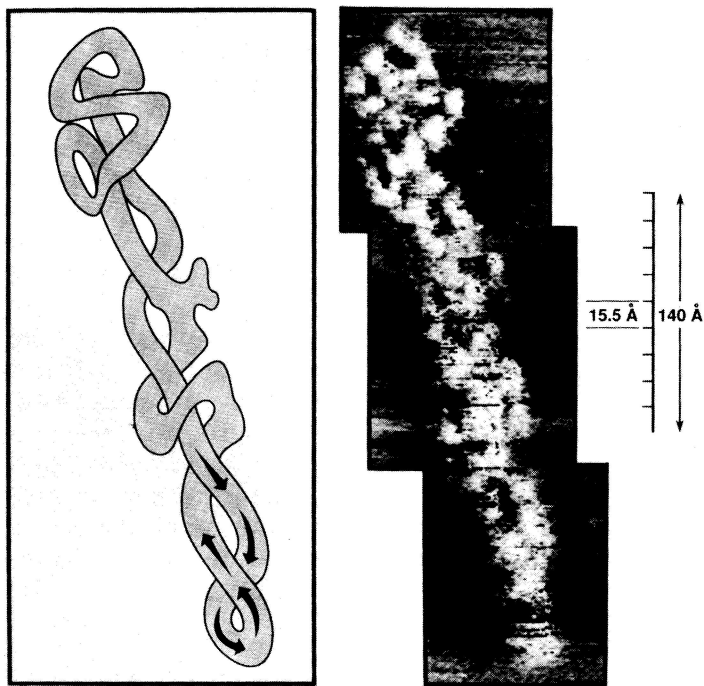


FIGURE 4B. Right side is a Mosaic gray-scale image composed of three overlapping, high-resolution STM images (dimension of one image: (140×140) \AA^2) showing a twisted poly-L-proline I helical chain. The 180° back-folding of the helical chain can clearly be seen at the bottom of the figure. The left side is an artist's rendering of the propagation of the helical chain as obtained from the STM image.

Examining a large number of such small aggregated molecules, we predominantly found such periodic structures which appear to be formed by parallel alignment of individual polypeptide chains. The distance between the two neighboring chains is approximately 25 Å. The lack of parallel line structures in the topmost aggregate in Figure 3, as found in most cases, is probably due to direct tip contact to the topmost aggregate and to poor electric conductivity of the sample. At present, no detailed fine-structures along the individual chains can be resolved, and therefore, we cannot identify the conformation of poly-L-proline solely from the helicity of the chains in the aggregates. We note, however, that the lack of sharp bends of the polypeptide chains strongly suggests the presence of poly-L-proline II. This is supported by the comparison of the specific rotation (-446°) of our poly-L-proline sample to that of poly-L-proline II (-540°) (5–10).

Figure 4 shows a feature that we occasionally observed and which is clearly different from those shown in Figures 2 and 3. In Figure 4A, we show the corresponding low-magnification, edge-detected STM image. The right side of Figure 4B is a mosaic gray-scale STM image consisting of three over-lapping, high resolution STM images, each one with the dimensions of $140 \text{ \AA} \times 140 \text{ \AA}$. The left side of Figure 4B illustrates the propagation of the helix chain which apparently reverses direction, at the bottom of the image, making a 180° turn (12).

We clearly observe a twisted and single-stranded poly-L-proline helix chain. We note that at the top part of Figure 4, the periodic structure of the molecules can be easily seen. The length of the repeating unit cell is 18.9 Å and the average width of the chain is 13 Å. These STM data are in excellent agreement with available X-ray data (pseudo-hexagonal unit cell: $c = 19.0 \text{ \AA}$ and $a = 9.05 \text{ \AA}$) for poly-L-proline I.

One major difference between poly-L-proline I and II, as evident from our images, is that poly-L-proline I is extremely flexible and shows a sharp bend along the propagation of the helix and even backfolds onto itself (see bottom part of Figure 4). This observation confirms a prediction, which was published by Edsall in 1954, that the presence of proline residues in the *cis* configuration can produce a sharp bend of a helix thereby reversing the direction of its axis by folding around this bend (12).

At present, the aggregation of air-dried poly-L-proline helices is not completely understood. We note that such aggregation phenomena have been previously reported by other investigators (13) and were interpreted in terms of tip interference based on the weak bonding between the molecule and the substrate. Such an interpretation, however, cannot explain the regular shape, the uniform size, and the random orientation of the aggregates that we observed in our experiments. We believe that the aggregation occurs at the final stage of the drying process where the surface tension of final liquid droplets tends to confine the helical chains. Furthermore, the interaction between the helical chains may cause the parallel alignment of the chains to form ordered structures.

Conclusions

We have presented high-resolution STM images of poly-L-proline which reveal the existence of two fundamentally different conformational structures of the poly-L-proline helix. Poly-L-proline I is relatively rigid and poly-L-proline II is very flexible. The capability to be able to identify two different conformations of poly-L-proline with STM, as demonstrated by the present study, should allow us in the future to study the mutarotation between

forms I and II of poly-L-proline in the presence of a variety of solvents. We note that sample deformation due to the direct tip contact becomes only significant when many overlapping polypeptide chains are present. Therefore, from our present STM studies on the successful imaging of single-stranded, unstacked poly-L-proline molecules, we believe that in future studies the technique of STM will allow us to resolve even the detailed atomic structure of the two different repeating unit cells of poly-L-proline molecules.

This work was partially supported by the National Science Foundation, the Welch Foundation and the Texas Higher Education Coordinating Board.

References

1. Gould, S., Marti, O., Drake, B., Helleman, L., Bracker, C.E., Hansma, P.K., Keder, N.L., Eddy, M.M. and Stucky, G.D. (1988) *Nature* 332:332.
2. Jericho, M.H., Blackford, B.L., Dahn, D.C., Frame, C. and Maclean, D.J. (1990) *J. Vac. Sci. Technol. A*8:663.
3. Lindsay, S.M., Thundat, T., Naghara, L., Knipping, U. and Rill, R.L. (1989) *Science* 244:1017.
4. Salmeron, M., Beebe, T., Odriozola, J., Wilson, T., Ogletree, D.F. and Siekhaus, W. (1990) *J. Vac. Sci. Technol. A*8:635.
5. Blout, E.R., Bovey, F.A., Goodman, M. and Lotan, N. (1974) In: *Peptides, Polypeptides and Proteins*, (E.R. Blout *et al.*, eds), J. Wiley and Sons, New York, pp. 26–189.
6. Caswell, D.S. and Spiro, T.G. (1987) *J. Am. Chem. Soc.* 109:2796.
7. Chao, Y.H. and Bersohn, R. (1987) *Biopolymers* 17:2761.
8. Isemura, T., Okabayashi, H. and Sakakibara, S. (1968) *Biopolymers* 6:307.
9. Madison, V. and Shellman, J. (1970) *Biopolymers* 9:511.
10. Traub, D.W. and Shmueli, U. (1963) *Nature* 198:1165.
11. Clemmer, C.R. and Beebe, Jr., T.R. (1991) *Science* 251:640.
12. Edsall, J.T. (1954) *J. Polym. Sci.* 12:253.
13. Lee, G., Arscott, P.G., Bloomfield, V.A. and Evans, D.F. (1989) *Science* 244:475.

Received May 25, 1994;
accepted July 15, 1994.